MRS Communications

Early Career Materials Researcher Prospective

Check for updates

Recent advances in integrated capture and electrochemical conversion of CO_2

Yongjun Kwon, and Binhong Wu, Gene and Linda Voiland School of Chemical Engineering and Bioengineering, Washington State University, Pullman, WA 99164, USA

Ning Zhang, Department of Earth and Environmental Engineering, Columbia University, New York 10027, USA

David Hand, Gene and Linda Voiland School of Chemical Engineering and Bioengineering, Washington State University, Pullman, WA 99164, USA

Tianyou Mou, and Xue Han, Department of Chemistry, Brookhaven National Laboratory, Upton, NY 11973, USA

Qiaowan Chang [ORCID]**,** Gene and Linda Voiland School of Chemical Engineering and Bioengineering, Washington State University, Pullman, WA 99164, USA

Address all correspondence to Qiaowan Chang at **qiaowan.chang@wsu.edu**

Abstract

Capturing and electrochemically converting carbon dioxide (CO_2) from industrial point sources, such as flue gas, is a promising approach to mitigate the greenhouse effect and protect the environment. However, these processes are characterized by high energy consumption and low energy efficiency, which need optimization. This prospective article provides a summary of the current strategies for capturing and electrochemically converting dilute CO_2 into valuable products. We will summarize strategies for capture and electrochemical reduction of CO_2 in a dilute stream, compare the advantages and disadvantages of using amines, membranes, alkaline solutions, and molten salts for CO_2 capture and conversion, and discuss the effects of CO_2 concentrations and typical impurities in flue gas (NO_x, SO_x, and O_2) on the performance of electrochemical CO_2 conversion. We will also provide an outlook on future opportunities for developing integrated processes for capturing and electrochemically converting CO_2 to valuable products.

Introduction

The increasing demand for energy has resulted in the emission of CO_2 from point sources, such as flue gas, which contains high levels of CO_2 that contribute to global warming and pose a threat to the ecosystem.[1,2] Therefore, it is urgent to address this environmental issue, which has provided an incentive for researchers to develop less carbon-intensive technologies and utilize alternative feedstocks. There has been significant research progress on converting CO_2 to value-added products, but these processes typically require pure CO_2.[3] The purification processes for obtaining concentrated and pure CO_2 involve energy-intensive capture techniques.[4] These carbon capture methods are expensive, costing around 40 to 120 US dollars per ton of CO_2.[5] As a result, there is a growing interest in direct utilization of CO_2 from flue gas. This approach avoids the need for traditional CO_2 purification processes, such as absorption and stripping columns, which are commonly used in other CO_2 capture methods.[6] However, there are two primary challenges in utilizing flue gas as the feed for CO_2 conversion: (1) The average CO_2 concentration in flue gas streams is dilute,[7,8] ranging from 5 to 15%.[9] (2) The flue gas stream contains impurities that are detrimental to the catalysts for CO_2 conversion. Both issues will be discussed in this Prospective article.

At present, extensive efforts have been devoted to the development of carbon capture and conversion (CCC) technologies, with thermochemical techniques being a typical example.

Current commercial techniques utilize amines to capture CO_2 and convert it into syngas ($CO + H_2$) through thermocatalytic reactions. However, the Carnot-like efficiency constrains thermochemical carbon capture. This, in turn, results in additional energy waste and substantial heating, which further contributes to energy expenditure.[10,11] Electrochemical CCC enables the utilization of clean power derived from green energy sources to capture and convert CO_2, thereby reducing energy costs.[12] From the perspective of energy efficiency, the Carnot-like energy penalty associated with the thermochemical CO_2 capture process can potentially be circumvented, leading to an improvement in energy efficiency.[10,11]

In this prospective, we summarize recent progress in combining CO_2 capture with the electrochemical conversion of CO_2 to valuable products, such as CO, formate, and solid carbon. We first discuss the electrochemical conversion of a dilute stream of CO_2, as well as the effects of common impurities in flue gas, such as NO_x, SO_x, and O_2, on the electrochemical performance. We then summarize and compare the common CO_2 capture technologies and their advantages in combining capture with conversion of CO_2. We conclude by providing an outlook on challenges and opportunities in integrating CO_2 capture and its electrochemical conversion.

Yongjun Kwon and Binhong Wu have contributes equally to this article.

Electrochemical CO$_2$ conversion with diluted CO$_2$ streams

The electrochemical CO$_2$ reduction reaction (CO$_2$RR) offers a sustainable method for converting CO$_2$ into valuable chemicals and fuels. Initial research and development efforts were primarily focused on using pure CO$_2$ gas as the reactant, with the goal of improving reaction conditions and catalyst performance to achieve maximum efficiency and product selectivity.[3] Over the past decade, significant progress has been made, leading to the identification of highly active and selective catalysts[13] and a comprehensive understanding of the underlying reaction mechanisms for CO$_2$RR.[14] With the advancement of CO$_2$RR processes, recent focus has turned towards using more easily accessible and economically viable sources of CO$_2$, particularly diluted CO$_2$ streams. These streams, which usually have CO$_2$ concentrations of 15% or less, are commonly found in industrial flue gases.[15] The transition to utilizing such diluted sources presents challenges for the current development of CO$_2$RR technologies, mainly due to the reduced concentration of CO$_2$ and the presence of various impurities, including O$_2$, NO$_x$, and SO$_2$. Therefore, it is imperative to develop innovative strategies for the design of electrolyzers and the development of efficient catalysts that maintain high levels of activity and selectivity, even under suboptimal conditions.

The type of electrolyzers, such as the H-cell, flow cell, and membrane electrode assembly (MEA), plays a key role in CO$_2$RR, and their design has a significant impact on efficiency and applicability.[16] H-cell electrolyzers, which consist of two half-cells separated by an ion-exchange membrane, are essential for fundamental study. This setup not only allows for precise control of the potential between working and reference electrodes, but also facilitates in-depth investigations when combined with *in-situ* spectroscopic techniques, such as Fourier transform infrared spectroscopy (FTIR)[17] and X-ray absorption spectroscopy (XAS).[18] These techniques enable the direct observation and analysis of the effects of applied potential on the structural evolution of catalysts, the formation of reaction intermediates, and the related reaction pathway. However, the scalability of the H-cell is typically limited by the solubility of CO$_2$ in an aqueous electrolyte, restraining the current density to only a few tens of mA cm^{-2}. Flow-cell electrolyzers are designed to optimize the introduction of gaseous CO$_2$ by utilizing a gas diffusion electrode (GDE), which improves mass transport and allows for higher current densities through continuous operations.[16] The focus of recent research is on integrating these systems with *in-situ* FTIR and Raman spectroscopy to understand the gas–liquid–solid interface.[16] This setup, while addressing the solubility issue, is sometimes challenged by high internal resistance and potential long-term stability concerns. To overcome this limitation, MEA-cell electrolyzers have been used.[16] Unlike H-cell and flow-cell electrolyzers, where the membrane acts merely as a separator,

in MEA-cell electrolyzers, it functions as a solid electrolyte. This minimizes the distance between the cathode and anode, significantly lowers the Ohmic resistance, and enhances energy efficiency, making MEA-cell electrolyzers promising for industrial applications.

When considering the utilization of diluted CO$_2$ sources from industrial emissions for CO$_2$RR, it is important to take into consideration the effect of impurities on electrolyzers, which cannot be overlooked. Although O$_2$ (4.3×10^{-5} g g^{-1} in water) is less soluble in water than CO$_2$ (1.7×10^{-5} g g^{-1} in water),[19] it is more readily reduced at the cathode, leading to the oxygen reduction reaction (ORR) and consuming electrons in the process. The ORR can compete with the desired CO$_2$RR in the cell, resulting in up to 99% of the current density being lost to the byproduct of ORR.[20] Van Daele et al. demonstrated that using a Bi$_2$O$_3$ catalyst did not impact the catalyst stability, but the CO$_2$RR Faradaic efficiency (FE) was affected by the competing ORR at 100 mA cm^{-2}.[21] O$_2$ can also alter the oxidation state of the catalyst and result in its corrosion. Davis et al. demonstrated that the solubility of O$_2$ increased as the concentration of KOH decreased under ambient conditions.[22] At higher O$_2$ solubility levels, catalysts such as the CuSn alloy may corrode at O$_2$ concentration between 0 and 2 ppm.[23] As a result, even small amounts of oxygen can potentially affect the performance of CO$_2$RR. To overcome these limitations, the use of hydrophilic supports like TiO$_2$ can help metallic catalysts, such as CuSn, maintain their oxidation state and CO$_2$RR selectivity.[7]

Another impurity, NO$_x$, is present in relatively low concentrations (below 200 ppm), but it poses challenges due to the solubility of NO$_x$ in water, resulting in the formation of acidic byproducts such as HNO$_3$ and HNO$_2$. These byproducts can significantly lower the pH in the electrolyzer, as demonstrated by Zhai et al.[24] In addition, NO$_x$ impacts the MEA performance; NO$_2$ concentrations exceeding 1667 ppm begin to poison the CuO catalyst, further compounded by the negative effect of O$_2$ (2000 ppm), which drastically reduces the CO$_2$RR FE of Cu catalyst by 12.4%.[24]

Similar to NO$_x$, the presence of SO$_2$ in the electrolyte leads to the formation of H$_2$SO$_3$, inducing acidic conditions that can reduce the pH to 4.0 or less. This induced acidity reduced both the FE and the production of C$_{2+}$ products, primarily because the selective reduction of SO$_2$ impedes the formation of these C$_{2+}$ products on Cu electrocatalysts.[25] However, the interaction of SO$_2$ with other catalyst materials, such as Sn and Ag, does not appear to impact the FE adversely. This is attributed to the thermodynamic instability of compounds like SnS$_2$ and Ag$_2$S during CO$_2$RR, which suggests that the negative effects of SO$_2$ are catalyst-dependent and can be mitigated through the careful selection of catalyst materials.[25]

Table I presents different catalyst types categorized into transition metals and main group metals, which are capable of utilizing diluted CO$_2$ directly for CO$_2$RR. Transition metals are commonly used as electrocatalysts and can be further

Table I. List of different catalyst systems.

Catalyst	Catalyst system configuration	CO_2 concentration percentage	Major product made	Selectivity	Partial current density (mA cm^{-2})	References
Ni–N/C	H-Cell	15%, 30%	CO	η_{CO}=91.6%	2.9	26
Pb	H-cell	4%, 15%, 25%, 50%, 80%, and 100%	Methyl formate	$\eta_{Methyl\ formate} \approx 42\%$	20	27
Ag	Flow cell	O$_2$ (0–20%) and small amounts of SO$_2$ and NO	CO	η_{CO}=92.35	100	21
Ag	Flow cell	10–100%	CO	η_{CO}=60% at 20% CO$_2$ concentration	100	28
Bi$_2$O$_3$	Flow cell	O$_2$ (0–20%) and small amounts of SO$_2$ and NO	Formate	$\eta_{formate} \approx 93.83\%$	100	21
SnO$_2$	Flow cell	10–100%	Formate	$\eta_{formate} \approx 82\%$	164	28
Ni–N/C	MEA	10%, 25%, 50%, 100%	CO	$\eta_{CO} = 93\%$	113.6	29
Ag	MEA	10%, 25%, 50%, 100%	CO	$\eta_{CO} = 69\%$	118.2	29

classified into noble metals and non-noble metals. As shown in Fig. 1(a), Van Daele et al. utilized an Ag solution that was spray-coated onto a gas diffusion layer to investigate the selectivity for CO in a flow cell without a CO_2 capture step.[21] To assess the catalyst stability, a CO_2 stream containing different impurities (NO$_x$, SO$_2$, and O$_2$) was introduced and the cell was operated for 20 h. The high FE of CO production (92.3%) was maintained, and the morphology and composition of the Ag catalyst remained unchanged, as evidenced by scanning electron microscopy (SEM) and energy dispersive spectroscopy (EDS) analyses, indicating the minimal impact of NO$_x$ and SO$_2$. Van Daele et al. also introduced different concentrations of O$_2$ (ranging from 0 to 20%) into the CO_2 stream to examine its effects on the Ag catalyst. Although O$_2$ had a negligible impact on the catalyst stability, the FE of CO significantly decreased from 95 to 13% as the O$_2$ concentration increased from 0 to 1% due to the competing ORR. In another experiment, Van Daele et al. used a flow cell setup with commercialized Ag nanoparticles tested in a CO_2 stream diluted from 80 to 10%.[28] The FE of CO decreased while the hydrogen evolution reaction (HER) and the formation of HCO$_3^-$ increased as the CO_2 composition dropped below 40%. Kim et al. compared a commercial noble metal nanoparticle, Ag, with a non-noble catalyst of Ni–N/C in an MEA cell [Fig. 1(b)].[29] The Ag catalyst exhibited a decrease in FE of CO from 94 to 40% as the CO_2 partial pressure decreased, whereas the Ni–N/C catalyst showed an increase in HER. However, the use of expensive noble metals like Ag has led to an increased demand for non-noble metals. An extensive study was conducted on the non-noble metal Ni–N–C, initiated by Jiao et al., who synthesized Ni–N/C single atom catalysts through pyrolysis of multivariate metal–organic frameworks (MTV-MOF) and embedded them into N-doped carbon as shown in Fig. 1(c).[26] The Ni–N/C catalyst was tested in an H-cell, demonstrating an FE of 96.8% for CO with pure CO_2. Subsequently, diluted CO_2 streams of 15% and 30% were introduced into the H-cell with Ni–N/C, resulting in an FE of 83.2% and 91.6% for CO, respectively.

A density functional theory (DFT) calculation was performed on the Ni–N–C catalyst to identify the formation of *COOH intermediate toward CO production. Kim et al. replicated the non-noble metal catalyst (Ni–N–C) and tested it in an MEA cell, where it maintained a high FE of CO even with declining CO_2 concentrations due to the low HER activity of Ni–N–C compared to the commercial Ag catalyst.[29]

Main group metals have also been explored for their potential to produce other valuable products from CO_2RR, such as formate. In Fig. 1(d), Gautam et al. used a commercial Pb foil in an H-cell with a methanol catholyte and flue gas.[27] Hofsommer et al. discovered the reaction mechanism to produce methyl formate over Pb foil, which proceeds as follows: the absorbed CO_2 reacts with 2 H$^+$ to form H$_2$CO$_2$; subsequently, H$_2$CO$_2$ reacts with CH$_3$OH to synthesize methyl formate.[30] While methanol reacts with CO_2 to form methyl formate (MF), the presence of SO$_2$ and NO had negligible effects on the FE of MF using Pb as the working electrode, which demonstrated excellent catalyst stability for 4 h. This is attributed to the resistance of Pb to the formation of surface sulfides. The presence of O$_2$ in the flue gas also increased the current density for MF production by promoting Pb oxide formation on the foil and suppressing the HER. However, Pb is a toxic element that can pose risks to human health, highlighting the need for safer materials. Van Daele et al. compared the CO_2RR performance between commercial SnO$_2$ and Ag in a flow cell.[28] They found that SnO$_2$ catalysts showed high FE for formate production, while Ag catalysts were more efficient for CO production. Salvini et al. showed that SnO$_2$ absorbs CO_2, which then produces *OCHO by reacting *CO$_2^-$ with H$^+$.[31] This reaction results in the synthesis of formate on SnO$_2$. Interestingly, as CO_2 concentrations decreased, SnO$_2$ maintained its selectivity for the formate, whereas Ag selectivity for CO decreased. This can be attributed to SnO$_2$ being less sensitive to lower CO_2 concentrations, a result of the different pH changes induced by CO and formate generated. Specifically, for CO production, it generates two OH$^-$ ions, which subsequently react with CO_2 to form HCO$_3^-$.
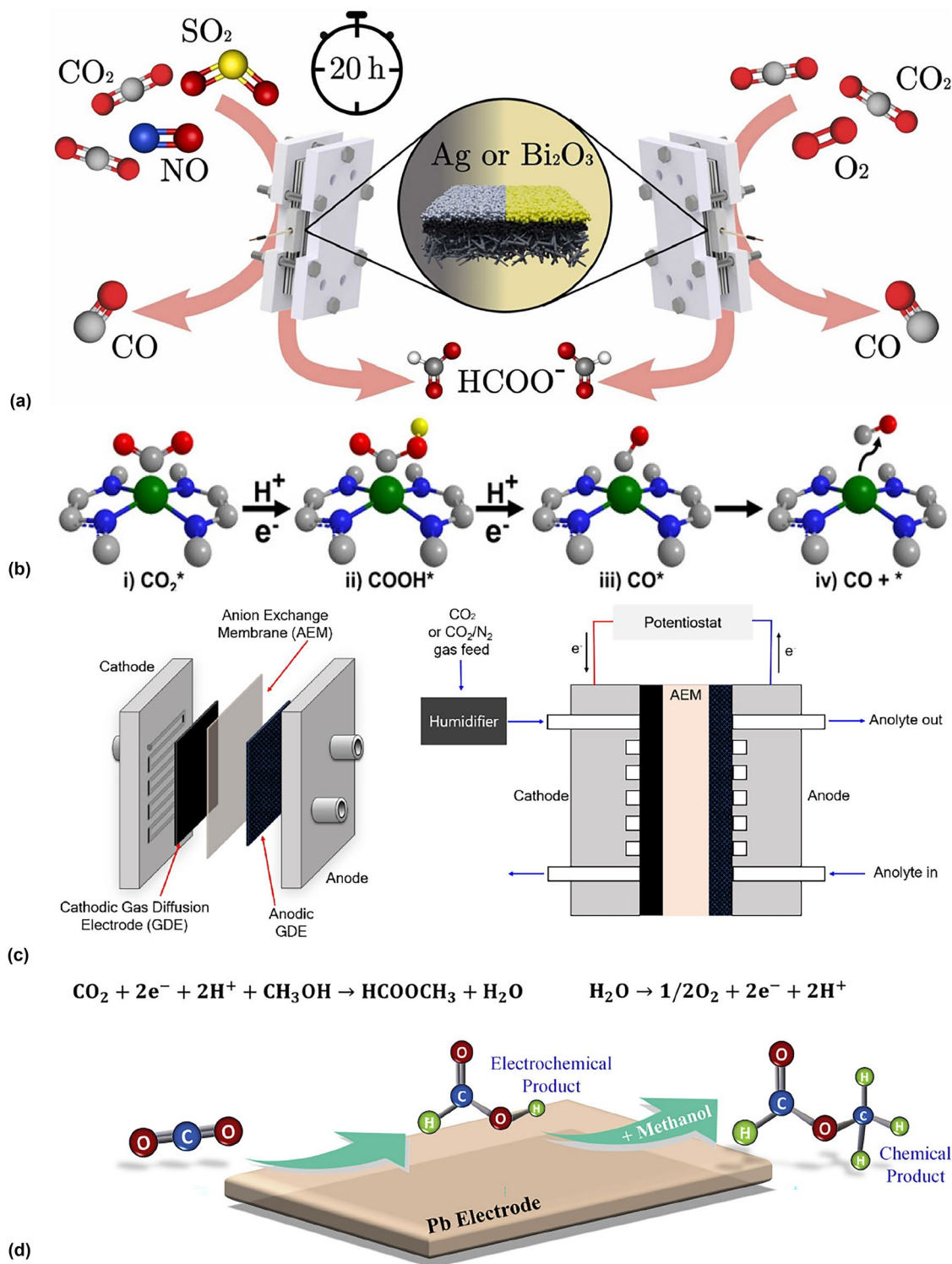
Figure 1. (a) Flow cell setup for Ag or Bi_2O_3. Reused from Van Daele et al.[21] (b) Reaction mechanism from Ni–N–C in an H-cell. Reused from Jiao et al.[26] (c) MEA-electrolyzer used for Ni–N–C and Ag. Reused from Kim et al.[29] (d) Reaction pathway involving Pb electrode in an H-cell. Reused from Gautam et al.[27]

In contrast, the production of $HCOO^-$ generates only one OH^-, which leads to less CO_2 neutralization. Van Daele et al. also used commercial Bi_2O_3 and Ag to test their stability under 20 h of electrolysis and observe their high FE for formate and CO in pure CO_2, respectively.[21] Feng et al. demonstrated the formation of key reaction intermediate *OCOH for the formation of formate on the Bi_2O_3 catalyst.[32] After the stability test in pure CO_2, they introduced different contaminants to simulate flue gas. It was found that SO_2 and NO had a negligible effect on the catalyst performance. However, the FE of formate for Bi_2O_3 decreased from 95 to 13%, and the FE of CO for Ag decreased from 91 to 5.7% due to the catalyst preference for ORR when 1% of oxygen contaminants were introduced into the feed stream.

Current strategies to integrate CO_2 capture with electrochemical CO_2RR

The utilization of diluted CO_2 streams in electrochemical CO_2RR lacks the CO_2 capture step to preconcentrate CO_2 from these diluted sources, resulting in lower efficiency for the utilization. To improve it, several innovative strategies have been developed. These methods are designed to integrate CO_2 capture directly with the electrochemical conversion process, enhancing the overall system capability to process diluted CO_2 streams effectively. Among these strategies, the use of amine-based solutions is noted for its ability to selectively bind CO_2, thus allowing its subsequent electrochemical conversion. Similarly, solutions containing OH^- and HCO_3^- have been explored for their dual role in capturing CO_2 and serving as a medium for its electrochemical conversion. Furthermore, molten salts act as a high-temperature capture medium suitable for integration with high-temperature electrolyzers such as molten salt CO_2 capture and electrochemical transformation (MSCC-ET), expanding the range of CO_2RR applications. In the following sections, we will discuss these methods in detail.

Using an amine-based solution as capture media

Amine-based CO_2 capture method relies on the chemical affinity of amines for CO_2 to selectively absorb CO_2 from gas streams *via* the formation of carbamate (Eq. 1). This process is reversible, enabling the captured CO_2 to be released for further utilization through heating or an electric field.[33] Previous research mainly focused on the separate processes of CO_2 capture and utilization, involving the concentration and transportation of CO_2 to conversion facilities in an energy-extensive way. However, some studies have demonstrated that directly using an amine solution for both the capture and electrochemical CO_2RR can significantly enhance energy efficiency. Chen et al. successfully converted CO_2 into CO and formate by using CO_2-saturated (30% wt.) amine solution as electrolyte [Fig. 2(a)] and In plate as electrode under -0.8 V vs. RHE, resulting in an FE of 4.8% and 2.4% for CO and formate, respectively.[34] However, the performance of the integrated process suffers from low FE because of the competition between HER and CO_2RR. To improve the FE of CO, cationic surfactant was explored in amine solutions to suppress HER, since the electrode surface with positive charge is not favorable to absorb H^+ for HER. For example, Chen et al. added 0.1 wt% cetyltrimethylammonium bromide (CTAB) into a CO_2-saturated amine solution, which improved the FE of CO from 4.8 to 17.0%, and the FE of formate from 2.4 to 45.4% at -0.8 V vs. RHE.[34] Beside cationic surfactant, electrode materials and structures also play key roles in determining the selectivity. Kim et al. used zeolitic imidazolate framework (ZIF)-8 with replaced Zn by Ni, achieving a boosted FE of 36% for CO in 1 M monoethanolamine at -0.8 V vs. RHE [Fig. 2(b)], while the Ag cathode only obtains 10% FE for CO.[35] Hossain et al. synthesized nano dendrites-based Ag electrode as a cathode for reducing CO_2 in 0.05 M ethanolamine, which yielded an FE of 36% for CO, compared to that of 6.74% for a smooth Ag cathode [Fig. 2(c)].[36]

$$2RNH_2 + CO_2 \leftrightarrow RNHCO_2^- + RNH_3^+ \tag{1}$$

The reaction pressure is another factor that impacts the selectivity and conversion rate. According to Diaz et al., both the FE and CO_2 conversion rate were improved when the pressure was increased from 0 to 40 psig with 0.2 M K_2SO_4 dissolved in 1-cyclohexylpiperidine-H_2CO_3 (CHP-H_2CO_3) solution as the capture-conversion electrolyte, from which the FE of CO increased from 16 to 32% at the current density of 104
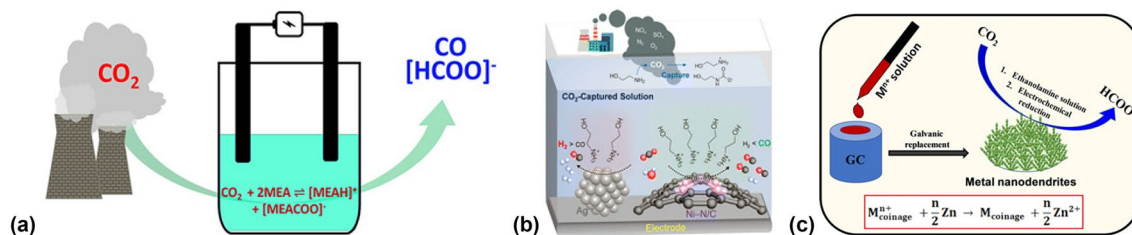

Figure 2. Illustrative diagram of amine solutions for CO_2 capture and electroreduction. (a) Directly using CO_2-saturated MEA solution to simulate the capture mediate for CO_2 electroreduction. Reused from Chen et al.[34] (b) (ZIF)-8 with Ni atoms and Ag cathodes for CO_2RR in MEA capture-conversion mediate. Reused from Kim et al.[35] (c) Metal dendrites as a cathode in EA capture-conversion mediate. Reused from Hossain et al.[36]

mA cm^{-2} and the conversion rate was improved from 28 to 72%.[37] Furthermore, the reaction temperature also influences the electrochemical performance during the reaction, due to the effect on kinetics and mass transport.[38] Pérez-Gallent et al. increased the reaction rate by a factor of 10 toward formate formation in 0.7 M tetrabutylammonium chloride containing 1 M 2-amino-2-methyl-1-propano preloaded with CO_2 in propylene carbonate solution at -2.5 V vs. Ag/AgCl on Pb cathode when the temperature was increased from 20 to 75°C.[39]

However, combining CO_2 capture with electrochemical CO_2RR also introduces complexity because CO_2 must be released at the anode and reduced at the cathode simultaneously. This integration is further impeded by the concentration of amines in the electrolyte, which can cause corrosion of metal catalysts and reduce electrode stability.[40,41] To overcome these issues, novel approaches must be developed that not only optimize pressure and temperature conditions, but also reduce the corrosive effects of amine-based capture media, resulting in a more effective and stable electrochemical CO_2 reduction process.

Using HCO$_3^-$/OH$^-$ containing solution as capture media

Alkaline solutions, including HCO_3^-, CO_3^{2-}, and OH^-, show possibilities of practical applications for integrated CO_2 capture and electrochemical reduction processes. Through reactions with OH^- ions, these solutions transform absorbed CO_2 into CO_3^{2-} or HCO_3^-, with HCO_3^- being a common electrolyte in electrochemical CO_2RR. For example, $KHCO_3$ solution is widely used as the electrolyte in many CO_2RR studies, emphasizing its effectiveness in this dual role.[42,43] In HCO_3^- electrolyte, the CO_2 reduced on the cathode either originates from the dissolved CO_2 or HCO_3^-, and the latter is identified as the predominant source of the CO reduction product by selectively labeling initial carbon sources ($^{13}CO_2$ and $H^{13}CO_3^-$).[44] The specific mechanisms behind the CO_2RR, whether originating from dissolved CO_2 molecules or HCO_3^- anions, remain a topic of ongoing debate,[45] which is not discussed in the current Prospective. A significant challenge when using solutions containing HCO_3^- directly for capture and electrolysis is the low current density due to the low CO_2 solubility. For example, Liu et al. applied a CO_2-saturated 0.1 M $KHCO_3$ solution as electrolyte with Ag nanocubes (NCs) as the cathode in an H-cell to produce CO with nearly 100% FE at -0.90V vs. RHE, but the current density was only 3.3 mA cm^{-2},[42] suggesting that low solubility of CO_2 limit its current density.

Therefore, the KOH solution is investigated to improve the current density, since it can capture more CO_2 to enhance its solubility. As depicted in Fig. 3(a), Ning et al. used a flow cell reactor filled with 1 M KOH as electrolyte and SnO$_2$/CuO NCs as the cathode, which presented a partial current density of formate of 310 mA cm^{-2} at -0.63V vs. RHE with corresponding FE exceeding 80%.[46] However, the carbon loss is significant during the conversion process due to the formation and crossover of carbonate, where the formed carbonate is carried
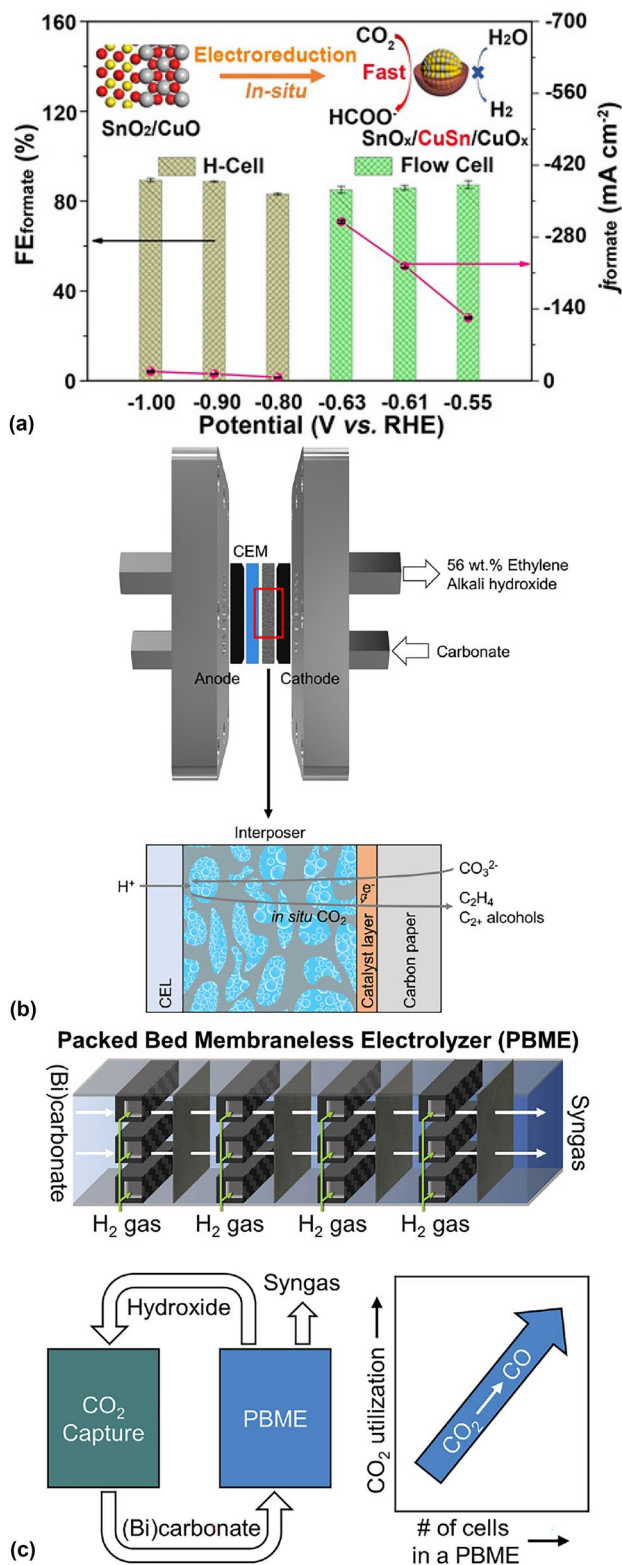

(a)

(b)

(c)

Figure 3. Illustrative diagram of HCO$_3^-$/OH$^-$ solutions for CO_2 capture and electroreduction. (a) Boosted current density in flow cell compared to that in H-cell. Reused from Ning et al.[46] (b) CEM coupled with interposer to achieve *in-situ* generation of CO_2 and reducing carbon loss. Reused from Lee et al.[47] (c) Membrane free technique for avoiding membrane degradation in alkaline solution. Reused from Peng et al.[48]

away with the electrolyte, resulting in 72% of the energy input being wasted.[49,50] Researchers also applied bipolar membrane (BPM) in the electrolyzer to reduce carbon loss, in which H_2O is able to split into H^+ and OH^- and diffuse to the cathode and anode chamber, respectively. The H^+ is able to react with CO_3^{2-} (Eq. 2) and *in-situ* generate CO_2 on the cathode.[51] For instance, Li et al. used a BPM as a separator [Fig. 3(b)], Ag as a cathode, and 1 M K_2CO_3 as a catholyte to simulate the capture-conversion electrolyte.[51] The study achieved 35% of full cell energy efficiency at 150 mA cm^{-2}, including 25% of FE for CO. Lee et al. utilized a cation-exchange membrane (CEM) coupled with the mixed cellulose ester (MCE) membrane, Cu/carbon paper as the cathode and 1 M K_2CO_3 as catholyte in a flow cell, in which the capture-and-electrolysis system sustains over 20 h at the current density of 200 mA cm^{-2}, with the C_{2+} FE in the range of 36–42%.[47] Although BPM is able to reduce the carbon loss, it decomposes in an alkaline solution. Designing a unique electrolyzer is another way to tackle this challenge. Figure 3(c) presents a multi-cell packed bed membrane-less electrolyzer (PBME) without membrane, in which Ag/CP was used as the cathode, 3 M $KHCO_3$ with 10 sccm was as the electrolyte and H_2 with 2.6 sccm was fed to each anode to generate H^+ to react with HCO_3^- forming CO_2, achieving up to 62% FE for CO with partial current density of 14 mA cm^{-2} and increasing CO_2 utilization from 12.9 to 20.5%.[48]

$$CO_3^{2-} + 2H^+ \rightarrow CO_2 + H_2O \qquad (2)$$
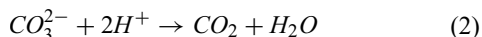
Even though BPM and PBME can mitigate the carbon loss to some extent, new issues arise such as dynamic changes in the pH value when H^+ flows through the BPM to the catholyte that might cause BPM decomposition, as well as inner impedance increasing from increased cell units. To overcome the difficulties mentioned above, future work should not only augment the solubility of CO_2 and suppress carbon loss, but also pay more attention to controlling the pH value to suppress HER, apply durable membranes, and design multiple-cell systems with lower inner impedance to optimize the capture-conversion electrolyte.

Using molten salt for CO_2 capture and electrochemical conversion

Molten salts have been recognized as promising materials for CO_2 capture, attributed to their distinctive properties such as high thermal stability, excellent ionic conductivity, and capability to dissolve various gas species including CO_2.[52,53] Molten salts are also utilized in molten salt CO_2 capture and electrochemical transformation (MSCC-ET). MSCC-ET, which is a specific form of electrolysis cells with molten salts as the electrolyte, enables their operation at high temperatures, typically ranging from 450 to 900°C. This high-temperature environment can electrochemically convert CO_2 into valuable chemicals and fuels, such as CO and synthetic carbon nanostructures. Thus, the use of molten salts facilitates the integration of CO_2 capture with electrochemical CO_2RR, making it a practical solution for

converting captured CO_2 into useful products. The most common carbonate-based salts, such as Li_2CO_3, K_2CO_3, and $BaCO_3$, are used as electrolytes due to their excellent solubility for CO_2 and high CO_2 capture efficiency.[54] Licht et al. used a Li_2CO_3 molten salts reactor at 750°C to generate solid carbon.[53]

The roles of molten salts include: effectively capturing CO_2 by the electrolyte by converting CO_2 into CO_3^{2-}, facilitating the transfer of ions, maintaining temperature in the cell by being chemically stable under high temperature, and the separation of products by synthesizing them into different phases.[54,55] Wang et al. discovered the mechanism of capturing and converting CO_2 using these molten carbonate salts at temperatures of 800°C.[55] They determined that Li_2CO_3 decomposes and becomes Li_2O, solid carbon, and O_2 (Eq. 3), due to the cathodic reaction described in Eq. 4. The O^{2-} is transferred to the anode, where the oxidation of O^{2-} to O_2 occurs.[54] As shown in Eq. 5, at high temperatures, Li_2O can further react with CO_2 in the atmosphere to become Li_2CO_3. The combination of the two reactions is represented in Eq. 6, where the carbon is deposited on the cathode and O_2 is formed at the anode. When the temperature exceeds 800°C, Meskine et al. discovered that CO formation occurs through reactions Eqs. 7 and 8, with Eq. 7 involving the use of dissolved CO_2 as the reactant, while Eq. 8 involving the reduction of CO_3^{2-}.[56]
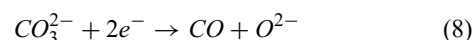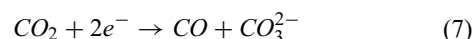
$$Li_2CO_3 + 4e^- \rightarrow C + Li_2O + O_2 \qquad (3)$$

$$CO_3^{2-} + 4e^- \rightarrow C + 3O^{2-} \qquad (4)$$

$$Li_2O + CO_2 \rightarrow Li_2CO_3 \qquad (5)$$

$$CO_2 + 4e^- \rightarrow C + O_2 \qquad (6)$$

$$CO_2 + 2e^- \rightarrow CO + CO_3^{2-} \qquad (7)$$
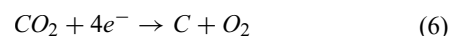
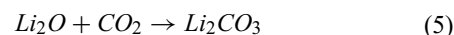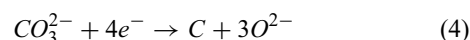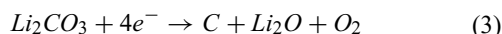$$CO_3^{2-} + 2e^- \rightarrow CO + O^{2-} \qquad (8)$$

Table II summarizes research efforts focusing on three primary objectives: synthesizing specific carbon nanomaterials using both flue gas and pure CO_2 streams;[57–61] expanding the synthesis of other chemicals, such as CO, in molten salt CO_2 electrochemical reactions;[62] and enhancing the performance by increasing the temperature of the electrolyzer.[63,64]

The demand for solid carbon has increased, due to the wide range of usage with carbon powder in batteries, thermocatalysis, and other applications.[65,66] Molten salts can use CO_2 to increase the production of carbon powders. Chen et al. employed a Li_2CO_3–Na_2CO_3–K_2CO_3 solution, a commercial Ni sheet as the cathode, and a commercial SnO_2 electrode as the anode in a molten salt reactor, successfully converting flue gas containing SO_2 and CO_2 into sulfur-doped carbon.[57] The CO_2 is captured by Li_2O, which reduces it to elemental carbon. SO_2 is also captured by Li_2O, forming Li_2SO_4 and effectively reducing SO_2 emissions. Under cathodic polarization, Li_2SO_4 undergoes electrochemical reactions to synthesize sulfur or sulfide, promoting the synthesis of sulfur-doped carbon on the cathode electrode.

Table II. Studies of molten salt electrolysis using CO_2 to convert into other carbon products.

| Cathode	Anode	Electrolyte	Temperature (°C)	Major product made	Current density (mA cm^{-2})	References
Ni	SnO_2	Li_2CO_3–Na_2CO_3–K_2CO_3–Li_2SO_4	475	S-doped carbon	281.25	57
Ni	SnO_2	Li_2CO_3–Na_2CO_3–K_2CO_3–Li_2SO_4	475–825	Graphite	1500	63
Galvanized steel	Ni	Li_2CO_3–Na_2CO_3–K_2CO_3	770	Carbon nanotubes	200	64
Ni	Pt–Ti	Li_2CO_3–Na_2CO_3–K_2CO_3	450	Electrolytic carbon	100	58
NiO–Co_3O_4	$Ni_{10}Cu_{11}Fe$	Li_2CO_3–Na_2CO_3–K_2CO_3	650	NiCo@g-C powder	10	59
Glassy carbon	Ni	Li_2CO_3–Na_2CO_3–K_2CO_3	450	Carbon powder	Not specified at -2.4 V vs. CO_2–O_2	60
Au wire	Carbon rod	LiF–NaF–Na_2CO_3	670	Carbon powder	0.316 to 1.121	61
Ti	Graphite	Li_2CO_3	900	CO	1000	62
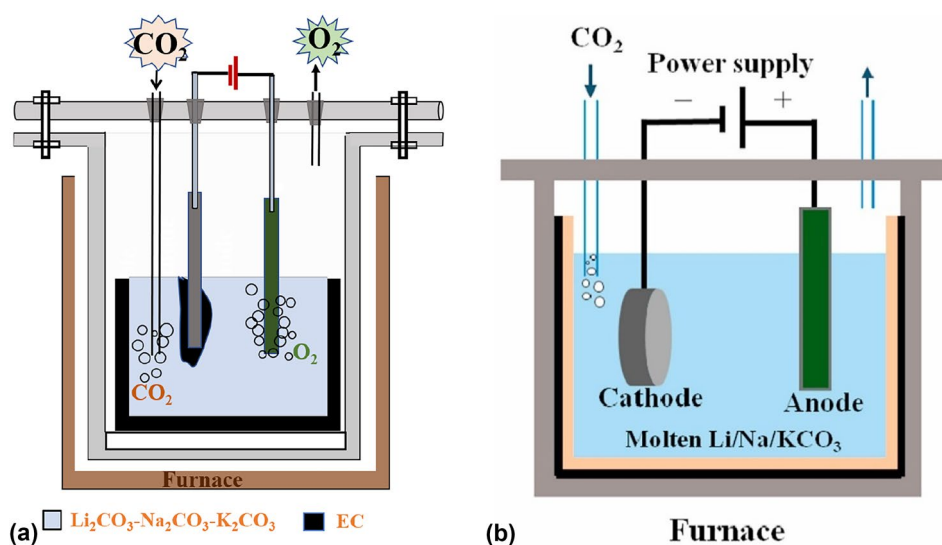
Figure 4. Illustrative diagram of molten salt reactors for CO_2 capture and electroreduction: (a) Molten salt reactor using a Ni cathode electrode with EC products and PtTi anode. Reused from Yang et al.[58] (b) Molten salt reactor with NiO–Co_3O_4 cathode and $Ni_{10}Cu_{11}Fe$ anode. Reused from Yu et al.[59]

Although Chen et al. used simulated flue gas, many catalyst systems in Table II use pure or diluted CO_2 as their feed stream. Figure 4 illustrates diagrams for molten salt reactor systems with pure CO_2. In Fig. 4(a), Yang et al. synthesized electrolytic carbon from CO_2 using Ni sheets and Pt/Ti plates in a Li_2CO_3, Na_2CO_3, and K_2CO_3 molten salt reactor, using a pure CO_2 feed stream.[58] The FE of electrolytic carbon for this system is unclear. The nickel alloy catalysts have also been explored. Yu et al. synthesized a core–shell structure catalyst of NiO–Co_3O_4,[59] demonstrating the conversion of captured CO_2 from pure CO_2 streams into graphite on the cathode surface. This is illustrated in Fig. 4(b). Due to the inherent poor stability of transition metals at high temperatures, researchers have explored alternative electrodes, such as carbon and Au, in molten salts. Groult et al. synthesized carbon powder using a glassy carbon as the cathode, Ni as the anode, and Li_2CO_3–Na_2CO_3–K_2CO_3 as the electrolytes.[60] The carbon

powder was utilized in a Li-ion battery, which had a reversible capacity of 1080 mAh g^{-1}. Massot et al. used an Au electrode to observe activity in alkaline fluoride media at temperatures ranging from 670 to 750°C, achieving the production of 1.8 wt% of carbon on the Au electrode at 720°C.[61]

To gain a better understanding of the effects of flue gas in molten salts, it is necessary to conduct studies at high temperatures. Lubomirsky et al. used a Ti cathode and graphite anode with Li_2CO_3 electrolyte, achieving 100% FE for CO at 900°C.[62] 2 mol% of SO_2 was added into the CO_2 feed stream, which produced CO and S on the cathode. However, the FE for CO decreased to 54% when adding SO_2 to the CO_2 feed.

The optimization of reactor design, such as temperature control and electrolyte mixture, can influence the distribution of products. Even though SO_2 limited the FE for CO production, Chen et al. observed that SO_2 could lower the temperature of graphitization, which typically occurs at 827°C in a

pure CO_2 stream.[63] Therefore, the temperature of the reactor is optimized to enhance the yield of this carbon product.[63] Chen et al. used a similar method to produce S-doped carbon.[57,63] They used a simulated flue gas and examined the yield of graphite between 425 and 825°C. The temperature was optimized at 775°C, as this temperature yielded the highest amount of graphite. Temperatures below 775°C caused a decrease in the graphite thickness of the formed S-doped carbon. Wu et al. also optimized their system by modifying the temperature and composition of the electrolyte mixture,[64] using a Li_2CO_3–Na_2CO_3–K_2CO_3 electrolyte with a galvanized steel cathode and Ni anode, operating at temperatures ranging from 577 to 770°C. This setup led to the synthesis of carbon nanotubes (CNT). At 770°C, the reactor yielded less than 15% of CNT. To enhance CNT production, Wu et al. tested three different electrolyte compositions at 770°C: Li_2CO_3, Li_2CO_3 + Na_2CO_3, and Li_2CO_3 + $BaCO_3$. It was observed that the CNT content significantly increased in pure Li_2CO_3, reaching over 85%. However, despite the increase in CNT production, the current efficiency was low (55%) due to CO production and other electrochemical reactions at high temperatures. In the Li_2CO_3–Na_2CO_3–K_2CO_3 system at 577°C, a current efficiency of 82% was achieved, but the yield was not specified.

Although the molten salt system synthesizes valuable carbon products, there are some challenges with MSCC-ET. This includes: the impurities from flue gas and the OER electrodes being unstable at high temperatures. While Lubomirsky et al. demonstrated that a flow of SO_2 can reduce the CO FE, there is a lack of data regarding other impurities, such as NO_x, in molten salt reactors.[62] Even in the absence of impurities, the materials used in the electrodes have not yet demonstrated stability under the harsh conditions of molten salts, which include extreme values of pH and high temperature, over extended periods. As a result, the presence of impurities could accelerate the deactivation rate and compromise catalyst stability. These challenging conditions pose scalability and corrosion issues for the equipment.

Another challenge is the synthesis of a stable and affordable anodic material. The anodic material in MSCC-ET is required for the OER to produce oxygen in molten salts. Ni-based catalysts have been widely used for this purpose. However, these anodes are unstable as Ni-based electrodes (Ni wire, Ni alloy) can be easily damaged by the electrolyte at high temperatures.[53,64,67] One solution is to use SnO_2 or Pt as the electrode, which should be inert to these harsh conditions.

Besides anode stability, mechanistic studies have been limited due to challenges in identifying the rate-determining step and reaction pathways in molten salts.[54,68] One way to determine the rate-determining step is to quantify the mass transfer of the oxygen ion during the reaction. To understand the reaction intermediates and mechanisms, *operando* characterizations (infrared or Raman spectroscopy) could provide useful information. DFT calculations can also provide insights into how the electric field affects the CO_3^{2-} capture and conversion.[54]

Conclusions and outlook

As illustrated in the examples above, integrated CO_2 capture and conversion processes show promise in the effective upgrading of CO_2 from dilute streams such as flue gas. In particular, the selection of the capture materials is critical in achieving the purification of CO_2 for the subsequent electrochemical conversion. The amine-based solutions, HCO_3^-/OH^- containing solution, and molten salt electrolytes have been explored as effective materials for CO_2 capture. The following capture materials should be explored to further optimize the effectiveness of the combined capture and electrochemical conversion strategies. Figure 5 illustrates the mechanism of these capture methods.

Using COF/MOFs as capture media

Covalent organic frameworks (COFs) are porous crystalline polymers with light-weight elements linked by strong covalent bonds, which lead to high porosity[72] and make them as promising sorption materials for CO_2 capture and conversion. For CO_2 capture, it requires designing COFs with high specific areas and more covalent bonds to interact with CO_2. For instance, Patel et al. synthesized N-rich COFs with a specific area up to 729 m^2 g^{-1}, achieving selectivity for capturing CO_2 72 times higher than N_2 under ambient conditions.[73] As for electrocatalysts, COFs decorated with transition metal atoms are able to achieve high FE for CO, which contribute to the low-coordination structure of the COF support, leading to intermediate species stabilized on the metal atoms, such as COFs decorated Ni atoms with FE of 90% for CO at −0.8 V vs. RHE.[69] Figure 5(a) depicts the ability of COFs to capture and electrochemically reduce CO_2, demonstrating that COFs are potential materials for integrated CO_2 capture and electroreduction.

Similarly, MOFs, which consist of metal ions or clusters interconnected by organic ligands, have also shown potential in this integrated approach. For instance, Liang et al. reported a Cu(II) MOF achieved a high volumetric capacity of 171 cm^3 cm^{-3} for CO_2 at 25°C, which is illustrated in Fig. 5(b).[70] In addition to CO_2 capture, MOFs have also been explored as electrocatalysts for CO_2, as reported that Cu rubeanate MOF is able to convert CO_2 to HCOOH with FE of 98% at −1.2V vs. SHE.[74] Other MOFs, such as Zn-MOFs, are capable of reducing CO_2 to CH_4.[75] The abilities of MOFs to capture and electrochemical convert CO_2 make them promising candidates for integrated dual functions. However, challenges such as low current density and poor stability still need to be addressed.

Using ionic liquids as capture media

Ionic liquids (ILs) have been widely investigated for their individual roles in CO_2 capture and CO_2 reduction processes. ILs can be classified into four groups: conventional IL, amino-functionalized IL, non-amino functionalized IL, and supported IL.[76] Conventional ILs consist of imidazolium anions and cations.[77] The CO_2 capture mechanism for these ILs involves physical dissolution, where CO_2 is attracted to imidazolium, but
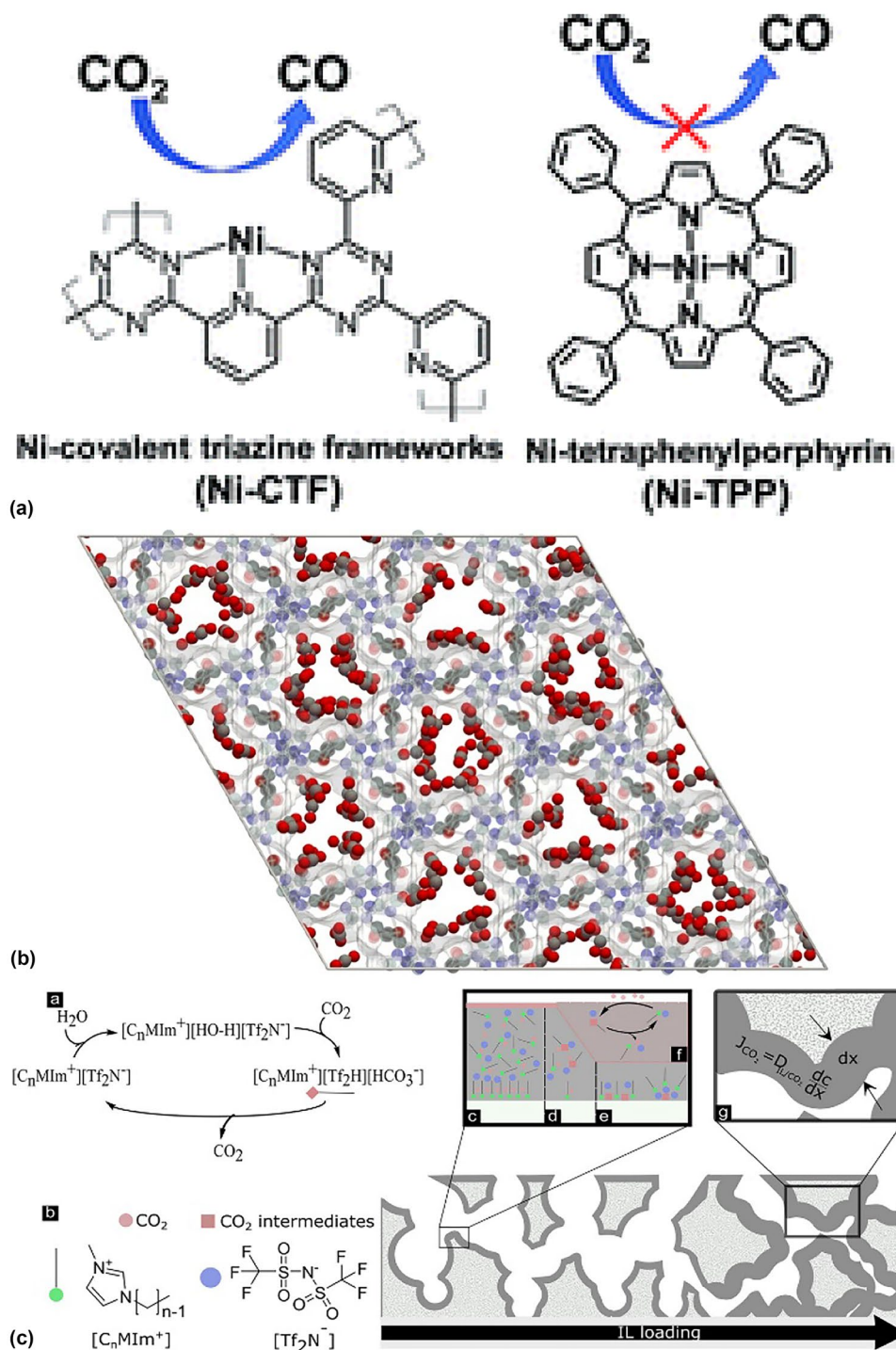
Figure 5. Mechanism schemes for: (a) Covalent triazine framework (COF) converting CO_2 to CO. Reused from Su et al.[69] (b) Cu(II)-MOF (FJI-H14) capturing CO_2. Reused from Liang et al.[70] (c) Hydrophobic imidazolium-IL to capture CO_2. Reused from Parada et al.[71]

the absorption capacity for CO_2 is low. To address this, Bates et al. utilized amino-functionalized ILs, where CO_2 is absorbed and desorbed on the NH_2 group, leading to an increases in the CO_2 absorption capacity.[78] However, the viscosity of the liquid increases due to hydrogen bonding on the NH_2 group,

which reduces the CO_2 mass transfer rate. One solution to overcome this challenge is the use of non-amino functional groups, utilizing N or O atoms in heterocyclic chemicals to avoid hydrogen bonding.[79] Another approach is the incorporation of supporting materials into amino-functionalized ILs,

forming supported ILs. Xue et al. introduced MCM-41 into a tetrabutylphosphonium 2-hydroxypyridine IL, resulting in an increased CO_2 absorption rate.[80] This enhancement is attributed to the porous support, which enhances gas–liquid contact and provides uniform IL dispersion. These IL compounds can be integrated with the electrochemical conversion of flue gas as they can mitigate competing electrochemical reactions, such as HER.

ILs can also enhance electrochemical CO_2RR efficiency by serving as electrolytes that reduce activation energy for CO_2 conversion, acting as electrolyte additives to enhance electrode catalytic activity, and modifying electrodes by optimizing the reaction microenvironment. Rosen et al. used an IL (1-ethyl-3-methylimidazolium tetrafluoroborate) that reduced the overpotential for the Ag electrode, which increased the FE of CO to 96% at 2.5 V vs. Ag/AgCl.[81] Neubauer et al. used an IL (1-ethyl-3-methylimidazolium trifluoromethane sulfonate) as an additive in the electrolyte, which had an FE for CO at 95.6% at 1.20 V vs. RHE.[82] In Fig. 5(c), Parada et al. used ILs based on hydrophobic imidazolium cations with an Ag foam, which increased CO FE from 65 to 85%.[71] Future studies to use ILs to integrate CO_2 capture and conversion should be explored.

Using quinone as capture media

Quinone-based materials are prominent for CO_2 capture. Li et al. detailed the capture mechanism using quinoline (QX) as an example.[83] The initial step involves the reduction of quinone at its reduction potential for CO_2 absorption on QX.[84] CO_2 then binds to the N atoms of quinone. To release the CO_2 from QX, the chemical undergoes an electrochemical oxidation cycle. Li et al. also discovered the potential of bifunctional azopyrinde-based quinones for carbon capture *via* an electrochemical method, achieving over 85% efficiency in a feed stream with 15% CO_2 and 5% O_2.[83] Besides capture, quinones, such as 2,5-ditert-butyl-1,4-benzoquinone (DBBQ), 9,10-anthraquinone (AQ), and 9,10-phenanthrenequinone, have been used by Wei et al.[85] as mediators in Li-CO_2 batteries in MeCN electrolyte to decrease the overpotential for CO_2 reduction. Among the quinones tested, DBBQ exhibited the lowest overpotential, as para-quinones demonstrated a stronger interaction with CO_2 compared to orthoquinone. Results from these studies demonstrate the potential to use quinone as a capture material, followed by its release to a catalyst electrode for CO_2 conversion.

Catalyst development and reactor optimization

In parallel with the exploration of CO_2 capture media, it is important to explore active, selective, and stable electrocatalysts for converting the captured CO_2 to valuable products, such as CO, formate, multi-carbon hydrocarbons, and solid carbons. It is also important to optimize the reactor configuration and the structural arrangement between the capture materials and electrocatalysts. The preferred capture-catalyst systems should be tolerant to dilute CO_2 concentrations and, to some extent, to impurities in the CO_2 stream. The effects of the operating temperature and pressure should also be investigated to identify process conditions that are optimal for using different CO_2 streams and for achieving specific conversion products.

Authors contributions

Y.J Kwon, B.H. Wu, and D. Hand performed the literature search and drafted the manuscript. N. Zhang revised the work. T.Y. Mou, X. Han proofread the work. Q.W. Chang conceived the idea for the article, drafted, and revised the work.

Funding

Data availability

Not applicable.

Declarations

Conflict of interest

On behalf of all authors, the corresponding author states that there is no conflict of interest.

References

1. A. Mikhaylov et al., Global climate change and greenhouse effect. Entrep. Sustain. Issues **7**, 2897–2913 (2020). https://doi.org/10.9770/jesi.2020.7.4(21)
2. A.M. Appel, J.Y. Yang, Maximum and comparative efficiency calculations for integrated capture and electrochemical conversion of CO_2. ACS Energy Lett. **9**, 768–770 (2024). https://doi.org/10.1021/acsenergylett.3c02489
3. Q. Lu et al., A selective and efficient electrocatalyst for carbon dioxide reduction. Nat. Commun. **5**, 3242 (2014). https://doi.org/10.1038/ncomms4242
4. G. Pipitone, O. Bolland, Power generation with CO_2 capture: technology for CO_2 purification. Int. J. Greenh. Gas Control **3**, 528–534 (2009). https://doi.org/10.1016/j.ijggc.2009.03.001
5. A. Baylin-Stern, N. Berghout, Is carbon capture too expensive? (2021). https://www.iea.org/commentaries/is-carbon-capture-too-expensive
6. I. Dimitriou et al., Carbon dioxide utilisation for production of transport fuels: process and economic analysis. Energy Environ. Sci. **8**, 1775–1789 (2015). https://doi.org/10.1039/c4ee04117h
7. Y. Xu et al., Oxygen-tolerant electroproduction of C_2 products from simulated flue gas. Energy Environ. Sci. **13**, 554–561 (2020). https://doi.org/10.1039/c9ee03077h
8. P.F. Hou et al., Well-defined single-atom cobalt catalyst for electrocatalytic flue gas CO_2 reduction. Small **16**, 2001896 (2020). https://doi.org/10.1002/smll.202001896
9. E. Worrell et al., Carbon dioxide emissions from the global cement industry. Annu. Rev. Energy Environ. **26**, 303–329 (2001). https://doi.org/10.1146/annurev.energy.26.1.303

10. J.W. Zhong et al., State of the art and perspectives in heterogeneous catalysis of CO_2 hydrogenation to methanol. Chem. Soc. Rev. **49**, 1385–1413 (2020). https://doi.org/10.1039/c9cs00614a

11. R.P. Ye et al., CO_2 hydrogenation to high-value products via heterogeneous catalysis. Nat. Commun. **10**, 5698 (2019). https://doi.org/10.1038/s41467-019-13638-9

12. Y. Pei, B. Zhang, Y. Lu, Carbon capture and utilization via electrochemistry, what's next? Next Nanotechnol. **3–4**, 100020 (2023). https://doi.org/10.1016/j.nxnano.2023.100020

13. H.P. Xu et al., Highly selective electrocatalytic CO_2 reduction to ethanol by metallic clusters dynamically formed from atomically dispersed copper. Nat. Energy **5**, 623–632 (2020). https://doi.org/10.1038/s41560-020-0666-x

14. H. Xiao, T. Cheng, W.A. Goddard, Atomistic mechanisms underlying selectivities in C_1 and C_2 products from electrochemical reduction of CO on Cu(111). J. Am. Chem. Soc. **139**, 130–136 (2017). https://doi.org/10.1021/jacs.6b06846

15. P. Bains, P. Psarras, J. Wilcox, CO_2 capture from the industry sector. Prog. Energy Combust. Sci. **63**, 146–172 (2017). https://doi.org/10.1016/j.pecs.2017.07.001

16. D.F. Gao et al., Designing electrolyzers for electrocatalytic CO_2 reduction. Acta Phys. Chim. Sin. **37**, 2009021 (2021). https://doi.org/10.3866/pku.Whxb202009021

17. J.E. Lee et al., In situ FTIR study of CO_2 reduction on inorganic analogues of carbon monoxide dehydrogenase. Chem. Commun. **57**, 3267–3270 (2021). https://doi.org/10.1039/d0cc07318k

18. D. Mendoza, S.T. Dong, B. Lassalle-Kaiser, In situ/operando X-ray spectroscopy applied to electrocatalytic CO_2 reduction: status and perspectives. Curr. Opin. Colloid Interface Sci. **61**, 101635 (2022). https://doi.org/10.1016/j.cocis.2022.101635

19. J.R. Partington, Tables of Physical and Chemical Constants and Some Mathematical Functions. By G.W.C. Kaye and T.H. Laby. J. Phys. Chem. **40**, 938–938 (1936). https://doi.org/10.1021/j150376a021

20. M. Wang et al., Acidic media enables oxygen-tolerant electrosynthesis of multicarbon products from simulated flue gas. Nat. Commun. **15**, 1218 (2024). https://doi.org/10.1038/s41467-024-45527-1

21. S. Van Daele et al., How flue gas impurities affect the electrochemical reduction of CO_2 to CO and formate. Appl. Catal. B **341**, 123345 (2024). https://doi.org/10.1016/j.apcatb.2023.123345

22. R. Davis, G. Horvath, C. Tobias, The solubility and diffusion coefficient of oxygen in potassium hydroxide solutions. Electrochim. Acta **12**, 287–297 (1967). https://doi.org/10.1016/0013-4686(67)80007-0

23. E.H. Greener, K. Matsuda, Effect of oxygen on the corrosion of dental amalgam. J. Oral Rehabil. **12**, 123–133 (1985). https://doi.org/10.1111/j.1365-2842.1985.tb00629.x

24. Y. Zhai, L. Chiachiarelli, N. Sridhar, Effect of gaseous impurities on the electrochemical reduction of CO_2 on copper electrodes. ECS Trans. **19**, 1 (2009). https://doi.org/10.1149/1.3220175

25. W. Luc et al., SO_2-induced selectivity change in CO_2 electroreduction. J. Am. Chem. Soc. **141**, 9902–9909 (2019). https://doi.org/10.1021/jacs.9b03215

26. L. Jiao et al., Single-atom electrocatalysts from multivariate metal–organic frameworks for highly selective reduction of CO_2 at low pressures. Angew. Chem. Int. Ed. **59**, 20589–20595 (2020). https://doi.org/10.1002/anie.202008787

27. M. Gautam et al., The effect of flue gas contaminants on electrochemical reduction of CO_2 to methyl formate in a dual methanol/water electrolysis system. Chem Catal. **2**, 2364–2378 (2022). https://doi.org/10.1016/j.checat.2022.08.001

28. S. Van Daele et al., Influence of the target product on the electrochemical reduction of diluted CO_2 in a continuous flow cell. J. CO_2 Util. **65**, 102210 (2022). https://doi.org/10.1016/j.jcou.2022.102210

29. D. Kim et al., Electrocatalytic reduction of low concentrations of CO_2 gas in a membrane electrode assembly electrolyzer. ACS Energy Lett. **6**, 3488–3495 (2021). https://doi.org/10.1021/acsenergylett.1c01797

30. D.T. Hofsommer et al., The pH and potential dependence of Pb-catalyzed electrochemical CO_2 reduction to methyl formate in a dual methanol/water electrolyte. ChemSusChem **15**, e202102289 (2022). https://doi.org/10.1002/cssc.202102289

31. C. Salvini et al., Active surface structure of SnO_2 catalysts for CO_2 reduction revealed by ab initio simulations. J. Phys. Chem. C **126**, 14441–14447 (2022). https://doi.org/10.1021/acs.jpcc.2c02583

32. X.Z. Feng et al., Bi_2O_3/BiO_2 nanoheterojunction for highly efficient electrocatalytic CO_2 reduction to formate. Nano Lett. **22**, 1656–1664 (2022). https://doi.org/10.1021/acs.nanolett.1c04683

33. I. Sullivan et al., Coupling electrochemical CO_2 conversion with CO_2 capture. Nat. Catal. **4**, 952–958 (2021). https://doi.org/10.1038/s41929-022-00734-1

34. L. Chen et al., Electrochemical reduction of carbon dioxide in a monoethanolamine capture medium. ChemSusChem **10**, 4109–4118 (2017). https://doi.org/10.1002/cssc.201701075

35. J.H. Kim et al., The insensitive cation effect on a single atom Ni catalyst allows selective electrochemical conversion of captured CO_2 in universal media. Energy Environ. Sci. **15**, 4301–4312 (2022). https://doi.org/10.1039/D2EE01825J

36. M.N. Hossain et al., Electrochemical reduction of CO_2 at coinage metal nanodendrites in aqueous ethanolamine. Chem. Eur. J. **27**, 1346–1355 (2021). https://doi.org/10.1002/chem.202003039

37. L.A. Diaz et al., Electrochemical production of syngas from CO_2 captured in switchable polarity solvents. Green Chem. **20**, 620–626 (2018). https://doi.org/10.1039/C7GC03069J

38. M. Li et al., Advancing integrated CO_2 electrochemical conversion with amine-based CO_2 capture: a review. Nanoscale **14**, 11892–11908 (2022). https://doi.org/10.1039/D2NR03310N

39. E. Pérez-Gallent et al., Integrating CO_2 capture with electrochemical conversion using amine-based capture solvents as electrolytes. Ind. Eng. Chem. Res. **60**, 4269–4278 (2021). https://doi.org/10.1021/acs.iecr.0c05848

40. V. Subramanian, W. Van Ooij, Effect of the amine functional group on corrosion rate of iron coated with films of organofunctional silanes. Corrosion **54**, 204–215 (1998). https://doi.org/10.5006/1.3284845

41. A. Veawab, P. Tontiwachwuthikul, A. Chakma, Corrosion behavior of carbon steel in the CO_2 absorption process using aqueous amine solutions. Ind. Eng. Chem. Res. **38**, 3917–3924 (1999). https://doi.org/10.1021/ie9901630

42. S.B. Liu et al., Unraveling structure sensitivity in CO_2 electroreduction to near-unity CO on silver nanocubes. ACS Catal. **10**, 3158–3163 (2020). https://doi.org/10.1021/acscatal.9b03883

43. S. Komatsu et al., Electrochemical reduction of CO_2 at Sb and Bi electrodes in $KHCO_3$ solution. Denki Kagaku oyobi Kogyo Butsuri Kagaku **63**, 217–224 (1995). https://doi.org/10.5796/kogyobutsurikagaku.63.217

44. D. Hursán, C. Janáky, Electrochemical reduction of carbon dioxide on nitrogen-doped carbons: insights from isotopic labeling studies. ACS Energy Lett. **3**, 722–723 (2018). https://doi.org/10.1021/acsenergylett.8b00212

45. X. Zhang et al., Electrocatalytic carbon dioxide reduction: from fundamental principles to catalyst design. Mater. Today Adv. **7**, 100074 (2020). https://doi.org/10.1016/j.mtadv.2020.100074

46. B. Ning et al., Derived CuSn alloys from heterointerfaces in bimetallic oxides promote the CO_2 electroreduction to formate. ChemElectroChem **8**, 1150–1155 (2021). https://doi.org/10.1002/celc.202100013

47. G. Lee et al., CO_2 electroreduction to multicarbon products from carbonate capture liquid. Joule **7**, 1277–1288 (2023). https://doi.org/10.1016/j.joule.2023.05.003

48. X. Pang et al., Membrane-free electrochemical CO_2 conversion using serially connected porous flow-through electrodes. Joule **6**, 2745–2761 (2022). https://doi.org/10.1016/j.joule.2022.11.003

49. A. Ozden et al., Cascade CO_2 electroreduction enables efficient carbonate-free production of ethylene. Joule **5**, 706–719 (2021). https://doi.org/10.1016/j.joule.2021.01.007

50. S. Park et al., High carbon efficiency in CO-to-alcohol electroreduction using a CO reservoir. Joule **7**, 2335–2348 (2023). https://doi.org/10.1016/j.joule.2023.08.001

51. Y.C. Li et al., CO_2 electroreduction from carbonate electrolyte. ACS Energy Lett. **4**, 1427–1431 (2019). https://doi.org/10.1021/acsenergylett.9b00975

52. R. Roper et al., Molten salt for advanced energy applications: a review. Ann. Nucl. Energy **169**, 108924 (2022). https://doi.org/10.1016/j.anucene.2021.108924

53. S. Licht et al., A new solar carbon capture process: solar thermal electrochemical photo (STEP) carbon capture. J. Phys. Chem. Lett. **1**, 2363–2368 (2010). https://doi.org/10.1021/jz100829s

54. R. Jiang et al., Advancements and potentials of molten salt CO_2 capture and electrochemical transformation (MSCC-ET) process. Curr. Opin. Electrochem. **17**, 38–46 (2019). https://doi.org/10.1016/j.coelec.2019.04.011

55. X.R. Wang et al., Magnetic carbon nanotubes: carbide nucleated electrochemical growth of ferromagnetic CNTs from CO_2. J. CO_2 Util. **40**, 101218 (2020). https://doi.org/10.1016/j.jcou.2020.101218

56. H. Meskine et al., Electrochemical investigations on CO_2 reduction mechanism in molten carbonates in view of H_2O/CO_2 co-electrolysis. Int. J. Hydrogen Energy **46**, 14944–14952 (2021). https://doi.org/10.1016/j.ijhydene.2020.07.008

57. Z.G. Chen et al., Flue-gas-derived sulfur-doped carbon with enhanced capacitance. Adv. Sustain. Syst. **1**, 1700047 (2017). https://doi.org/10.1002/adsu.201700047

58. J. Yang et al., A novel porous carbon derived from CO_2 for high-efficient tetracycline adsorption: behavior and mechanism. Appl. Surf. Sci. **538**, 148110 (2021). https://doi.org/10.1016/j.apsusc.2020.148110

59. R. Yu et al., A facile strategy to synthesize graphitic carbon-encapsulated core-shell nanocomposites derived from CO_2 as functional materials. Compos. Commun. **22**, 100464 (2020). https://doi.org/10.1016/j.coco.2020.100464

60. H. Groult et al., Lithium insertion into carbonaceous anode materials prepared by electrolysis of molten Li-K-Na carbonates. J. Electrochem. Soc. **150**, G67–G75 (2003). https://doi.org/10.1149/1.1531490

61. L. Massot et al., Studies of carbon nucleation phenomena in molten alkaline fluoride media. Electrochim. Acta **48**, 465–471 (2003). https://doi.org/10.1016/s0013-4686(02)00646-1

62. V. Kaplan, E. Wachtel, I. Lubomirsky, CO_2 to CO electrochemical conversion in molten Li_2CO_3 is stable with respect to sulfur contamination. J. Electrochem. Soc. **161**, F54–F57 (2014). https://doi.org/10.1149/2.052401jes

63. Z.G. Chen et al., Synthesis of nanostructured graphite via molten salt reduction of CO_2 and SO_2 at a relatively low temperature. J. Mater. Chem. A **5**, 20603–20607 (2017). https://doi.org/10.1039/c7ta06590f

64. H.J. Wu et al., One-pot synthesis of nanostructured carbon materials from carbon dioxide via electrolysis in molten carbonate salts. Carbon **106**, 208–217 (2016). https://doi.org/10.1016/j.carbon.2016.05.031

65. S. Yuan et al., Carbon-based materials as anode materials for lithium-ion batteries and lithium-ion capacitors: a review. J. Energy Storage **61**, 106716 (2023). https://doi.org/10.1016/j.est.2023.106716

66. R. VanderWal, M.M. Nkiawete, Carbons as catalysts in thermo-catalytic hydrocarbon decomposition: a review. C **6**, 23 (2020). https://doi.org/10.3390/c6020023

67. K.F. Du et al., Unusual temperature effect on the stability of nickel anodes in molten carbonates. Electrochim. Acta **245**, 402–408 (2017). https://doi.org/10.1016/j.electacta.2017.05.149

68. Q. Zhu, Y. Zeng, Y. Zheng, Overview of CO_2 capture and electrolysis technology in molten salts: operational parameters and their effects. Ind. Chem. Mater. **1**, 595–617 (2023). https://doi.org/10.1039/D3IM00011G

69. P. Su et al., Covalent triazine framework modified with coordinatively-unsaturated Co or Ni atoms for CO_2 electrochemical reduction. Chem. Sci. **9**, 3941–3947 (2018). https://doi.org/10.1039/C8SC00604K

70. L.F. Liang et al., Carbon dioxide capture and conversion by an acid-base resistant metal-organic framework. Nat. Commun. **8**, 1233 (2017). https://doi.org/10.1038/s41467-017-01166-3

71. W.A. Parada et al., CO_2 electroreduction on silver foams modified by ionic liquids with different cation side chain length. ACS Appl. Mater. Interfaces **14**, 14193–14201 (2022). https://doi.org/10.1021/acsami.1c24386

72. X. Feng, X. Ding, D. Jiang, Covalent organic frameworks. Chem. Soc. Rev. **41**, 6010–6022 (2012). https://doi.org/10.1039/C2CS35157A

73. H.A. Patel et al., Unprecedented high-temperature CO_2 selectivity in N_2-phobic nanoporous covalent organic polymers. Nat. Commun. **4**, 1357 (2013). https://doi.org/10.1038/ncomms2359

74. R. Hinogami et al., Electrochemical reduction of carbon dioxide using a copper rubeanate metal organic framework. ECS Electrochem. Lett. **1**, H17–H19 (2012). https://doi.org/10.1149/2.001204eel

75. X.C. Kang et al., Highly efficient electrochemical reduction of CO_2 to CH_4 in an ionic liquid using a metal-organic framework cathode. Chem. Sci. **7**, 266–273 (2016). https://doi.org/10.1039/c5sc03291a

76. X.W. An et al., Application of ionic liquids in CO_2 capture and electrochemical reduction: a review. Carbon Resour. Convers. **6**, 85–97 (2023). https://doi.org/10.1016/j.crcon.2023.02.003

77. Y. Hu et al., Experimental investigation of CO_2 absorption enthalpy in conventional imidazolium ionic liquids. Greenh. Gases Sci. Technol. **8**, 713–720 (2018). https://doi.org/10.1002/ghg.1777

78. E.D. Bates et al., CO_2 capture by a task-specific ionic liquid. J. Am. Chem. Soc. **124**, 926–927 (2002). https://doi.org/10.1021/ja017593d

79. C.M. Wang et al., Carbon dioxide capture by superbase-derived protic ionic liquids. Angew. Chem. Int. Ed. **49**, 5978–5981 (2010). https://doi.org/10.1002/anie.201002641

80. C.F. Xue et al., Unique allosteric effect-driven rapid adsorption of carbon dioxide in a newly designed ionogel [P_{4444}][2-Op]@MCM-41 with excellent cyclic stability and loading-dependent capacity. J. Mater. Chem. A **5**, 6504–6514 (2017). https://doi.org/10.1039/c6ta10693e

81. B.A. Rosen et al., Ionic liquid-mediated selective conversion of CO_2 to CO at low overpotentials. Science **334**, 643–644 (2011). https://doi.org/10.1126/science.1209786

82. S.S. Neubauer et al., Overpotentials and Faraday efficiencies in CO_2 electrocatalysis-the impact of 1-ethyl-3-methylimidazolium trifluoromethanesulfonate. Adv. Energy Mater. **6**, 1502231 (2016). https://doi.org/10.1002/aenm.201502231

83. X. Li et al., Redox-tunable lewis bases for electrochemical carbon dioxide capture. Nat. Energy **7**, 1065–1075 (2022). https://doi.org/10.1038/s41560-022-01137-z

84. F. Simeon et al., Electrochemical and molecular assessment of quinones as CO_2-binding redox molecules for carbon capture. J. Phys. Chem. C **126**, 1389–1399 (2022). https://doi.org/10.1021/acs.jpcc.1c09415

85. W. Yin et al., Electrochemical reduction of CO_2 mediated by quinone derivatives: implication for Li-CO_2 battery. J. Phys. Chem. C **122**, 6546–6554 (2018). https://doi.org/10.1021/acs.jpcc.8b00109